


PSFC/JA-00-30

**Resistive $n=1$ Modes in Reversed Magnetic Shear Alcator
C-Mod Plasmas**

View metadata, citation and similar papers at core.ac.uk

brought to you by  DSpace
provided by DSpace

J. Snipes, S. Wolfe, A. Bondeson¹

September 2000

Plasma Science and Fusion Center
Massachusetts Institute of Technology
Cambridge, MA 02139 USA

¹Chalmers University, Goteborg, Sweden.

This work was supported by the U.S. Department of Energy, Cooperative Grant No. DE-FC02-99ER54512. Reproduction, translation, publication, use and disposal, in whole or in part, by or for the United States government is permitted.

Submitted for publication to *Nuclear Fusion*.

October 10, 2000

**n=1 RESISTIVE MODES
in REVERSED MAGNETIC SHEAR
ALCATOR C-MOD PLASMAS**

Y. IN, J.J.RAMOS, A.E.HUBBARD, I.H.HUTCHINSON,
M. PORKOLAB, J. SNIPES, S. WOLFE, A. BONDESON[†]

MIT Plasma Science and Fusion Center

Cambridge, Massachusetts 02139

United States of America

[†] Chalmers University, Göteborg, Sweden

During current ramp-up discharges with early auxiliary RF heating, reversed magnetic shear profiles have been obtained on Alcator C-Mod. MHD oscillations are often observed on ECE diagnostics, as well as magnetics. Although no direct q -profile measurement was available, a hollow current density profile with $q_{\min}=2.5$ was reconstructed by EFIT. The location of the biggest electron temperature fluctuations was close to the outer $q = 3$ rational surface. Based on a resistive linear stability code (MARS), the MHD oscillations were identified as n=1 resistive “multiple” tearing modes. Since the pressure profile was hollow and $q > 1$ in the core, a resistive interchange mode was also predicted to be unstable at the inner $q = 4$ rational surface, despite the low β_N .

I. Introduction

Reversed magnetic shear profiles are predicted to give better performance¹ in terms of confinement, stability and self-sustaining bootstrap currents. Many experiments have since verified such predictions in various tokamaks.²⁻⁴ In particular, in the negative central magnetic shear (NCS) region, the plasma shows excellent stability to $n = \infty$ ideal magnetohydrodynamic (MHD) ballooning modes.⁵ However, when reversed magnetic shear plasmas are accompanied by MHD fluctuations, plasma performance is reduced. Understanding the characteristics of the MHD activity associated with reversed magnetic shear plasmas is required prior to adopting reversed magnetic shear operation as an advanced tokamak operation scenario.^{6,7}

A resistive MHD mode specific to reversed magnetic shear plasmas is a resistive double tearing mode, which can be destabilized when a pair of rational surfaces with the same q are close to each other. Since it is a global mode, it can be observed in experiments rather easily. For a single tearing mode,⁸ in a classical tearing theory, $\Delta' > 0$, where $\Delta' \equiv (\psi'/\psi)|_{r_s+w/2}^{r_s-w/2}$, is an unstable condition with magnetic island width (w) centered at $r=r_s$. In a neoclassical theory, even negative Δ' can be unstable in that transport and polarization terms should be also considered.⁹ On the other hand, for a double tearing mode,¹⁰⁻¹⁴ we do not have a similarly simple analytic criterion.

In addition, a pressure gradient driven resistive interchange mode might be observed near a rational surface in the NCS region. Since the resistive interchange mode is localized close to a resonant layer, it is not easy to observe in experiments unless other MHD modes are suppressed. Although resistive interchange modes in a tokamak were predicted in theory¹⁵ as early as resistive tearing modes, the experimental observation was only recently reported.¹⁶

A reversed magnetic shear configuration is generally created during current

ramp discharges because the current diffusion time ($\tau_R = \mu_0 a^2 / \eta$ where μ_0 : vacuum permeability [$4\pi \times 10^{-7}$ H/m], a : scale length, η : resistivity) is much longer than the plasma current rise time. If additional heating is launched at the early current ramp stage, it retards the current penetration further as τ_R is proportional to $T_e^{3/2}$, which helps to keep the reversed magnetic shear profiles. To achieve high performance reversed magnetic shear plasmas in Alcator C-Mod,¹⁷ ICRF heating is added to early ohmic plasmas as its auxiliary power, unlike most other tokamaks whose main power source is neutral beam injection (NBI).

II. Experiments

A. Diagnostics

The Alcator C-Mod is a high field ($B_T = 5\sim 8$ T), compact ($R \sim 0.67$ m, $a \sim 0.22$ m), diverted tokamak. Poloidal magnetic field pickup loops in Alcator C-Mod are used to measure MHD fluctuations, which are usually digitized at a rate of 1 MHz. For these studies, we use four sets of toroidally displaced coils located on outboard limiters. Two sets are composed of 7 coils and the others of 4 coils. In addition, there are some inboard coils which are located closer to the plasma, which are useful for determining poloidal mode numbers. For electron temperature measurements, Thomson scattering and ECE (electron cyclotron emission) diagnostics, including a Michelson interferometer, radiometer and grating polychromator (GPC), are installed on Alcator C-Mod. The Michelson interferometer is absolutely calibrated; all the other ECE temperature measurement diagnostics are cross-calibrated on the basis of the Michelson calibration. For the purpose of observing MHD activity on electron temperature measurements, the GPC was chosen as a main diagnostic because it provides good spatial resolution (~ 1 cm) and

temporal response (up to 2 μsec). The GPC is based on the extraordinary mode (X-mode) of emission at the second harmonic of the electron cyclotron frequency.

B. MHD observations

For Alcator C-Mod, a typical current ramp up rate is 5.0 MA/sec up to 0.1 sec. During the experiment discussed here, the current ramp up rate was initially 5.1 MA/sec and then was reduced to 1.5 MA/sec until the target current $I_p=0.8$ MA was reached. As shown in Fig. 1, there were short trips during the very early ICRF heating phase due to poor coupling to the plasma. The power was up to 1.5 MW during the period of the MHD activity, which was observed not only on magnetics, but also on GPC with the same coherent frequencies. The toroidal mode numbers (n) of all the MHD fluctuations on magnetics were identified as $n = 1$, while their poloidal mode numbers (m) decreased from 7 to 5 until the big MHD fluctuations were observed on Channel 6 of GPC ($R \sim 0.8$ m) around $t = 0.11$ sec (See Fig. 2). Using the EFIT¹⁸ program, the equilibrium associated with the MHD activity was reconstructed. An internal pressure profile was used as a constraint for EFIT, in addition to external magnetics data. Fig. 3 shows the evolution of the temperature fluctuations ($\Delta T \equiv (T_{max} - T_{min})/2$) around $t=108$ msec, while Fig. 4 shows the q -profile reconstructed by EFIT at $t=108$ msec.

For the pressure profile, $T_{i(e)}, n_{i(e)}$ ($i(e)$: ion (electron)) are needed. The electron temperatures (T_e) were given by GPC, while the ion temperature (T_i) is inferred based on a simple equilibration model which assumes that the electrons and ions are thermally equilibrated and that the ion confinement time is constant over the profile. The ion density profile ($n_i(R)$) was assumed

to be the same as $n_e(R)$. The densities (n_e) were inferred from Abel-inverted visible Bremsstrahlung from a multichord diagnostic whose view is horizontal and near the midplane.^{19,20} The brightness of the visible Bremsstrahlung diagnostic is a function of Z_{eff} , n_e , and T_e . When the electron temperatures (T_e) are provided from GPC and Z_{eff} is assumed to be a constant, n_e can be inferred. As a note, the inverted density profile obtained from far-infrared (FIR) interferometry is regarded as less reliable for this analysis. This is due primarily to the vertical view of the diagnostic, which passes cold, relatively dense plasma in the vacuum chamber above and below the main plasma. Since the contributions of the edge plasmas to the FIR line integrated density measurements are not separated from those of the main plasma, the inversion process is sensitive to rather arbitrarily assumed edge plasma densities. For this reason, the horizontal visible Bremsstrahlung diagnostic was preferred for density measurement. Therefore, the pressure profile is given by $P = n_e T_e + \sum n_i T_i \sim n_e (T_e + T_i) \leq 2n_e T_e$, where n_e is inferred from visible Bremsstrahlung brightness, while T_e is measured by GPC.

The dashed curve of Fig. 5 is the pressure profile calculated in the aforementioned way. Based on this internal pressure profile, as well as magnetics, a most likely reversed magnetic shear configuration has been reconstructed during the current ramp stage. Based on the reconstructed equilibrium, the MHD stability at $t=108$ msec will be discussed.

III. Interpretation

For stability analysis, the MARS code²¹ has been used. This is a linear resistive MHD stability code with a given toroidal mode number and we consider $n = 1$, which has been ascertained in magnetics unambiguously. For the input parameters, the Lundquist number (or magnetic Reynolds number

S_0) and the shape of the temperature profile are needed. Unless otherwise specified, in the following case $S_0 \equiv (\tau_R/\tau_A)_0 = 1.67 \times 10^7$ is used, where τ_A is the Alfvén time. The shape parameter ($\eta_i \equiv d(\ln T)/d(\ln n)$) has been determined from the relation between density ($n(\psi)/n_0 = (P(\psi)/P_0)^{1-\alpha}$) and temperature ($T(\psi)/T_0 = (P(\psi)/P_0)^\alpha$), so $\eta_i = \alpha/(1 - \alpha)$. Since the density profile was rather flat, a best fit for α was found to be $\frac{6}{7}$, giving $\eta_i = 6.0$.

The first distinguishable mode has resistive double tearing-like behavior, as shown in Fig. 6. When the magnetic Reynolds number is increased (in other words, η , which is inversely proportional to S_0 , decreases), such an instability disappears, which indicates that it is a non-ideal (resistive) mode. Around the $q = 3, 4$ rational surfaces, there were big pressure fluctuations, whose mode components are represented by different symbols (e.g. $\bullet(m = 3), \diamond(m = 4)$). Also, near each resonant surface, each mode component changes its phase. When all of the components are summed up, the pressure fluctuation (δp) theoretically predicted in the MARS code is peaked near the outer $q = 3$ rational surface, whose radial location is 83.5 cm ($\rho \sim 0.73$) (See the red dash-dot curve and solid thick black curve of Fig. 6). Since other resonant layers are seen at various rational surfaces, the instability can be called a resistive “multiple” tearing mode. In comparison with the experimental observations shown in Fig. 3, the location of the peaked fluctuations predicted in the MARS code is less than 2-3 cm away from the Channel 6 ($R = 80\text{-}81$ cm ($\rho \sim 0.62$)), whose ΔT is the biggest. In addition, a range of possible q profiles is shown by the solid thin black curves, while other thick short and long dashed curves show other reconstructed q -profiles based on different constraints. From these profiles, the outer $q=3$ surfaces ($\rho \sim 0.7$) are much closer to the location of the peak ΔT_e channel. Considering that the potential errors in determining the q -profile via EFIT reconstruction are not insignificant, the theoretical result based on the solid thick q -profile seems to

match the experimental observation quite well. Since this “multiple” tearing mode is a global mode, it is not surprising that most of the GPC channels showed large or small electron temperature fluctuations in the experiment. The perturbed magnetic flux $(\Delta b)^{21}$ linear eigenfunction is shown in Figure 7. According to the MARS code results, $\gamma\tau_A \sim 1.8 \times 10^{-4}$, where γ is the growth rate [sec^{-1}] and $\tau_A \sim 8 \times 10^{-8}$ sec. Thus, the growth time is approximately 0.44 msec, which is within a typical range of tearing mode evolution.

Interestingly, the MARS code also predicted a non-global mode, whose fluctuation is highly localized near one of the $q=4$ rational surfaces in the NCS region. It was predicted as a resistive interchange mode. This would be difficult to observe without suppressing all the other global MHD instabilities, apart from the capability of spatially well-resolved diagnostics. This resistive interchange mode is contrasted with those found in DIII-D experiments.¹⁶ According to the DIII-D results, the resistive interchange instability can occur beyond a threshold β_N^1 . However, the β_N of the equilibrium discussed here was $0.27[\%mT/MA]$, which is low. Basically, this instability was predicted to occur due to a hollow pressure profile, not from high β_N . Since the elongation ($\kappa \sim 1.14$) during the current ramp was close to one, we could assume a circular plasma. The ideal (Mercier) stability criterion ($D_I < 0$)² was satisfied. In this case, the H-factor³ in the NCS region was no more than -0.02. Since $|H| = 0.02 \ll 1/2$ and $(q^2 - 1)$ was positive, the

¹ $\beta_N \equiv \beta/(I_p/aB_0)$ [% m T/MA]; $\beta = 2\mu_0 \langle p \rangle / B_0^2$, I_p : plasma current [MA], a : minor radius [m], B_0 : magnetic field at magnetic axis [T], and $\langle p \rangle$: volume averaged pressure [Pa]

²According to Glasser, Greene and Johnson,¹⁵ $D_I = -1/4 + 2ap'/(B_s^2 S^2)(q^2 - 1)$

$$H = \frac{\mu_0 p' V' f}{2\pi q'} \left[\left\langle \frac{1}{|\vec{\nabla}\psi|^2} \right\rangle - \frac{\langle B^2 / |\vec{\nabla}\psi|^2 \rangle}{\langle B^2 \rangle} \right]$$

, where $p' = dp/d\psi$, $V' = dV/d\psi$, $q' = dq/d\psi$, $\langle \cdot \rangle$: flux surface average quantity and $\vec{B} = f\nabla\phi + \nabla\phi \times \nabla\psi$.

resistive interchange mode stability criterion ($D_R < 0$)⁴ was violated by the positive sign of p' . In more recent discharges, there were some indications of highly localized T_e fluctuations that we believe have occurred due to such a resistive (or possibly ideal) interchange mode. The temperature fluctuations appeared on only one of the GPC core channels in a discharge with a hollow T_e profile. Detailed analysis is under way and will be reported separately.

IV. Conclusions

During current ramp discharges of reversed magnetic shear experiments, MHD oscillations have been observed on ECE, as well as on magnetics. The toroidal mode number was identified as $n = 1$ unambiguously, while the poloidal mode number decreased from 7 to 5 until the biggest T_e fluctuation was observed near the outer $q = 3$ rational surface. The equilibrium of the reversed magnetic shear configuration was reconstructed by EFIT. Using a linear resistive MHD code (MARS), its stability has been analysed. The MHD activity of the T_e measurements was identified as an $n = 1$ resistive “multiple” tearing mode. This code gave $\gamma\tau_A \sim 1.8 \times 10^{-4}$ and the growth time was predicted to be approximately 0.44 msec.

Another $n=1$ resistive mode has been predicted in NCS region of the reversed magnetic shear plasma. Its driving force comes from inverted pressure gradient ($p' > 0$) in the core which violates the resistive interchange mode stability criterion ($D_R < 0$). Although the associated magnetic island size is challenging to Alcator C-Mod diagnostic capabilities, there were some indications of highly localized fluctuations on GPC in other recent discharges which seemed to have been caused by the resistive interchange mode.

⁴ $D_R = D_I + (H - 1/2)^2$. In particular, if $|H| \ll 1/2$, $D_R \simeq D_I + 1/4 \simeq 2ap'/(B_s^2 S^2)(q^2 - 1)$

In summary, the global MHD mode during reversed magnetic shear experiments of Alcator C-Mod has been ascertained as $n=1$ resistive “multiple” tearing mode. In addition, a resistive interchange mode in NCS region of low β_N has been predicted due to a hollow pressure profile.

Acknowledgements

The authors would like to thank E. Marmor for providing density profiles using visible Bremsstrahlung diagnostic and M. Greenwald for helpful discussion regarding pressure profiles. This work has been supported at MIT by USDOE Contract No. DE-FC02-99ER54512.

References

- ¹KESSEL, C., MANICKAM, J., REWOLDT, G., and TANG, W. M., Phys. Rev. Lett. **72** (1994) 1212
- ²LEVINTON, F. M. et al., Phys. Rev. Lett. **75** (1995) 4417
- ³STRAIT, E. J. et al., Phys. Rev. Lett. **75** (1995) 4421
- ⁴The JET Team, Plasma Phys. and Controlled Fusion **39** (1997) B353
- ⁵GREENE, J.M. and CHANCE, M.S., Nucl. Fusion **21** (1981) 453
- ⁶TURNBULL, A.D., TAYLOR, T.S., LIN-LIU, Y.R., and ST. JOHN, H., Phys. Rev. Lett. **74** (1995) 718
- ⁷TAYLOR, T.S., Plasma Phys. and Controlled Fusion **39** (1997) B47
- ⁸FURTH, H.P., KILLEEN, J. and ROSENBLUTH, M.N., Phys. Fluids **6** (1963) 459
- ⁹LA HAYE, R.J., SAUTER, O., Nucl. Fusion **38** (1998) 987
- ¹⁰WHITE, R.B., MONTICELLO, D.A., ROSENBLUTH, M.N. and WADDELL, B.V., *Plasma Physics and Controlled Fusion Research 1977* (IAEA, Vienna, 1977), Vol.1, 569
- ¹¹CARRERAS, B., HICKS, H.R. and WADDELL, B.V., Nucl. Fusion **19** (1979) 583
- ¹²PRITCHETT, P.L., LEE, Y.C. and DRAKE, J.F., Phys. Fluids **23** (1980) 1368
- ¹³CHANG, Z. et al., Phys. Rev. Lett. **77** (1996) 3553

- ¹⁴GÜNTER, S. et al., Nucl. Fusion **39**, special issue, (1999) 1793
- ¹⁵GLASSER, A.H., GREENE, J.M. and JOHNSON, J.L., Phys. Fluids **19** (1976) 567
- ¹⁶CHU, M.S. et al., Phys. Rev. Lett. **77** (1996) 2710
- ¹⁷PORKOLAB, M. et al., Proceedings of the 24th EPS Conf on Contr. Fusion and Plas. Phys. **Part II**, (1997) 569
- ¹⁸LAO, L.L. et al., Nucl. Fusion **30** (1990) 1035
- ¹⁹FOORD, M.E., MARMAR, E.S. and TERRY, J.L., Rev. Sci. Instru. **53** (1982) 1407
- ²⁰CHRISTENSEN, C., PhD thesis, MIT, 1999
- ²¹BONDESON, A., VLAD, G. and LÜTJENS, H., Phys. Fluids B**4** (1992) 1889

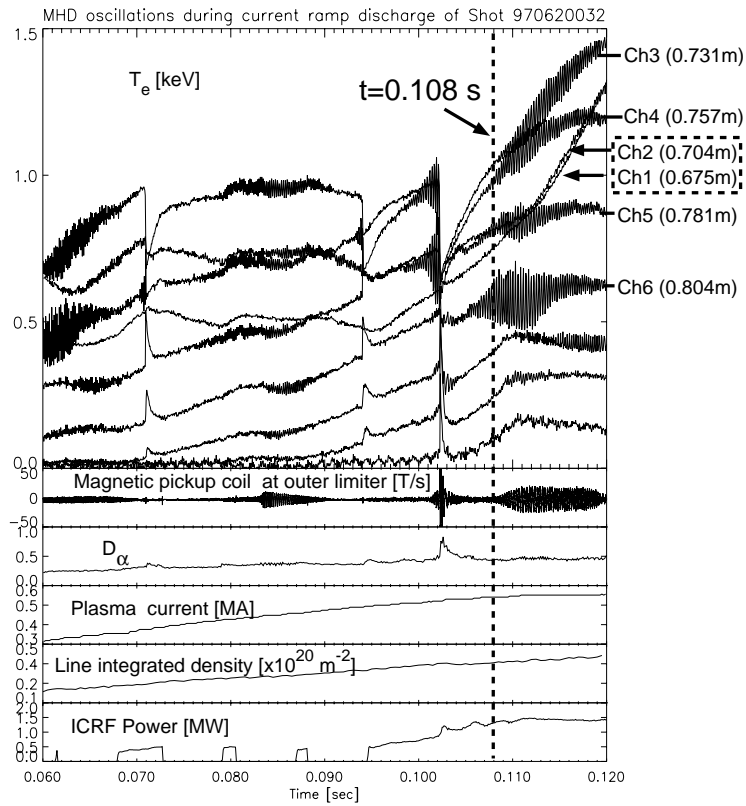


Figure 1: MHD activity during reversed magnetic shear plasma. Note that the electron temperatures of the two innermost channels are lower than the third channel (i.e. a hollow temperature profile).

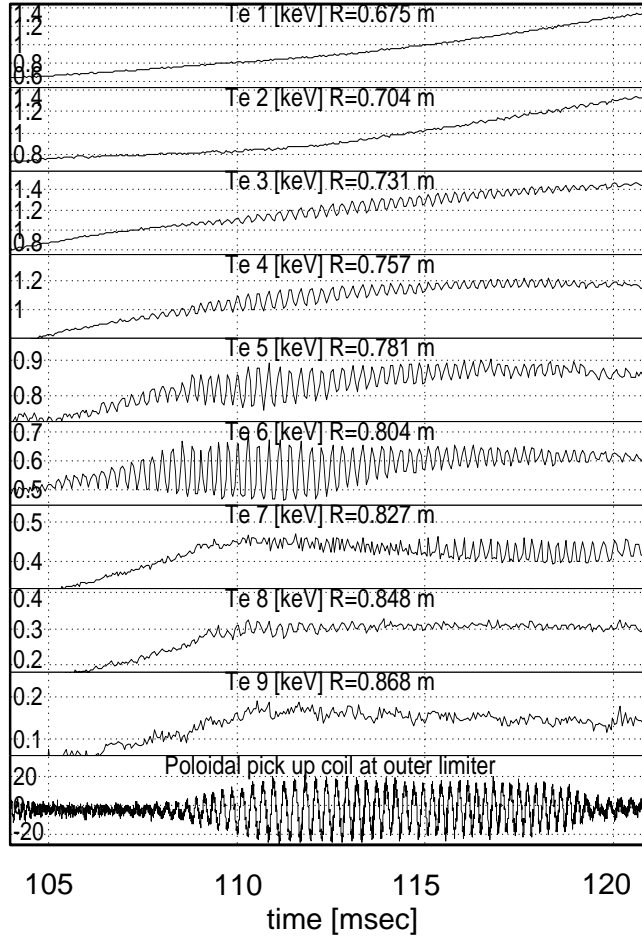


Figure 2: Enlarged view of the MHD activity observed on GPC and magnetics of Fig. 1 near $t=108$ msec. In particular, observe that the T_e fluctuations on Channel 6 are the biggest and that the oscillation frequency ($3 \sim 4$ kHz) is the same as that of the magnetics.

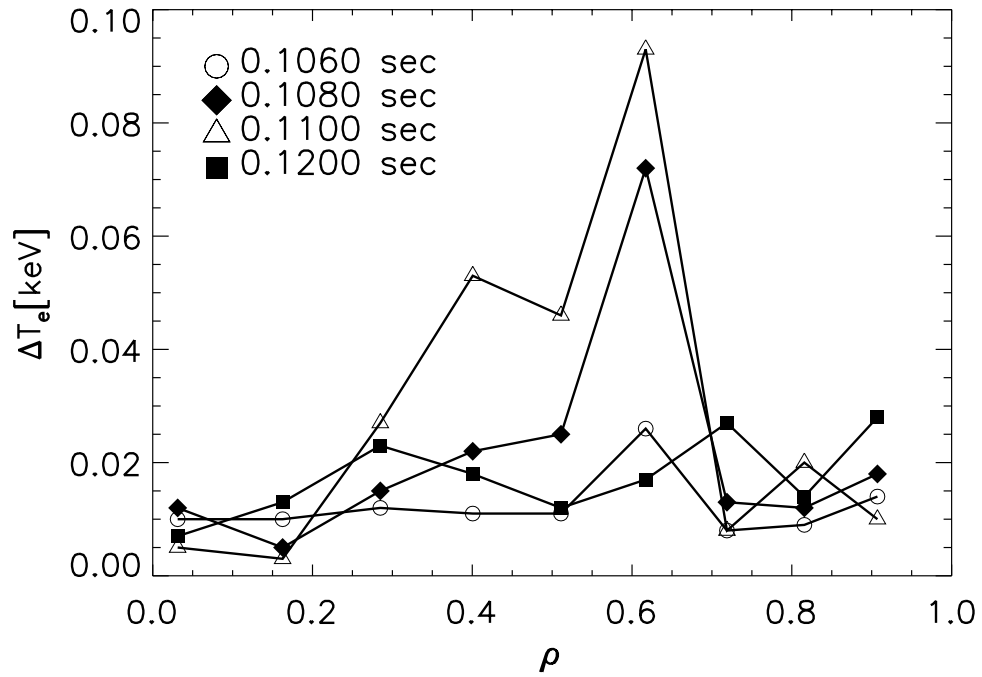


Figure 3: At $t=0.108$ sec considered here, Channel 6, which is located at $R=80 \sim 81$ cm ($\rho \sim 0.62$), shows the biggest fluctuations. Also, note that the fluctuations of Channel 6 evolve, peak near $t=0.11$ sec and then the biggest fluctuations move outward into Channel 7 ($R \sim 83$ cm) at $t=0.120$ sec.

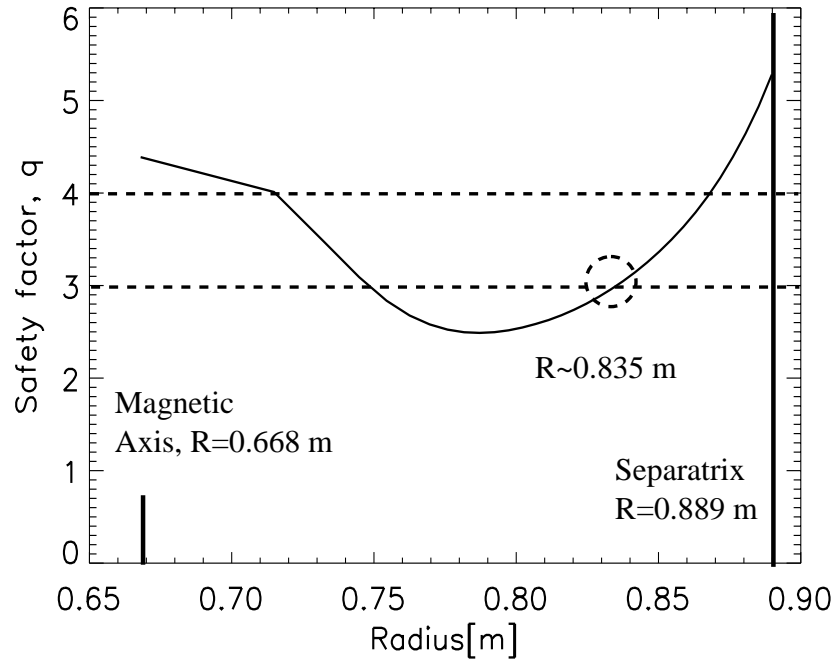


Figure 4: q -profile at $t=108$ msec. Note that the $q=3$ outer rational surface is located at $R \sim 83.5$ cm ($\rho \sim 0.73$), which is close to $(\Delta T)_{max}$.

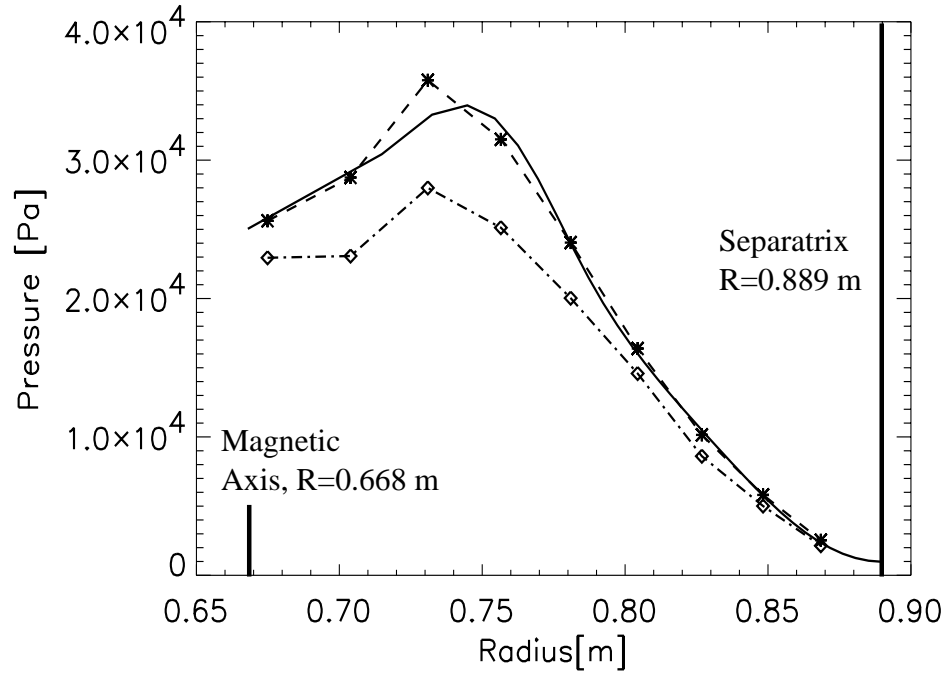


Figure 5: Pressure profiles: Solid curve - from EFIT reconstruction; Dashed curve - calculated from T_e of GPC and n_e inferred from visible Bremsstrahlung; Dash-dot curve - $2 \times (n_e T_e)$, based on T_e of GPC and n_e from TCI-inversion using routinely given EFIT reconstruction.

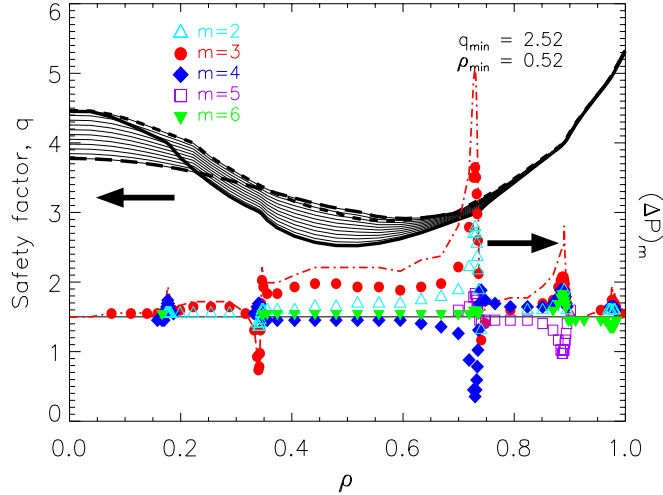


Figure 6: Perturbed pressure eigenfunction for the $n=1$ resistive “multiple” tearing mode. When all the components are summed up, the total predicted pressure fluctuations (δp) are delineated with the red dash-dot curve. Note that resonant layers are observed not only at the outer $q = 3$ surface, but also at the inner $q = 3$ and at the $q = 4$ rational surfaces, which characterizes the “multiple” tearing mode. This can be compared with the temperature fluctuations (ΔT_e) of $t=0.108$ sec in Fig. 3. Theory and experiment results match each other. The growth rate for this mode is $\gamma\tau_A \sim 1.8 \times 10^{-4}$ for $S_0 = 1.67 \times 10^7$, where τ_A : Alfvén time $\sim 8 \times 10^{-8}$ sec. The local Lundquist number S at the outer $q = 3$ surface is 6.15×10^6 . The other two cases, whose q -profiles are shown in thick short and long dashed black curves respectively, also predicted almost the same fluctuations.

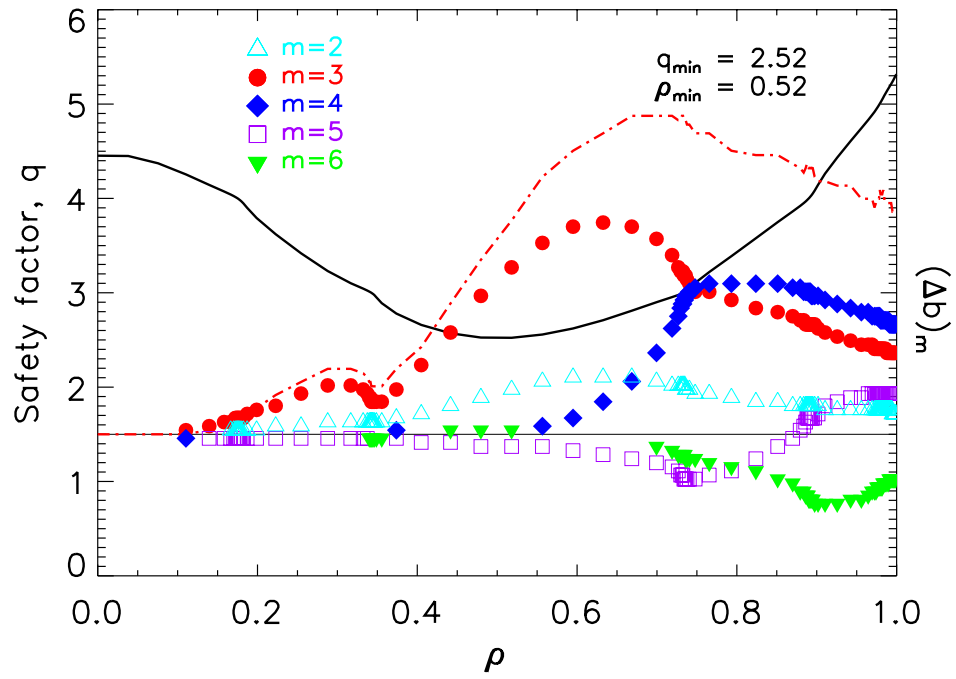


Figure 7: Perturbed radial magnetic flux defined as $\Delta b \equiv \frac{d\Phi}{d\theta d\phi} = [\nabla\psi \cdot (\nabla\theta \times \nabla\phi)]^{-1} \tilde{\mathbf{B}} \cdot \nabla\psi$. The sum of the Fourier components giving the perturbed magnetic flux at $\theta = 0$ is delineated with the dash-dot curve.